Journal of Chromatography, 126 (1976) 369–380

CHROM. 9423

A FLOW CONTROLLER FOR HIGH-PERFORMANCE LIQUID CHROMATOGRAPHY AND ITS APPLICATIONS

KEI ASAI, YOH-ICHI KANNO, AKIRA NAKAMOTO and TASUKU HARA
Scientific and Industrial Instrument Division, Shimadzu Seisakusho Ltd., Kyoto 604 (Japan)

SUMMARY

A new flow control system has been developed for high-performance liquid chromatography, which consists of a flow sensor (a bubble flow tube) connected to the detector outlet, an electro-pneumatic controller and a pressure control valve for a pneumatic amplifier pump.

The flow sensor measures the volumetric flow-rate of the carrier from the column with no influence of viscosity changes. The system keeps the flow-rate of the carrier constant within an accuracy of $\pm$ 0.3%.

A high-performance liquid chromatograph equipped with this flow controller provides various advantages:

(1) The repeatability of the retention time and peak area is better than $\pm$ 0.5%, even in gradient elution analysis.

(2) The flow-rate is set digitally with no calibration factor for any type of carrier.

(3) The real flow-rate is indicated every few seconds on a recorder or a meter.

(4) Calibration procedures involved in gradient rate changes can be eliminated.

INTRODUCTION

High-performance liquid chromatography (HPLC) has become a very important technique in analytical chemistry, and the repeatability and the accuracy of the results obtained are becoming increasingly important.

One of the important parameters that affects the analytical accuracy is the flow-rate of the carrier. The causes of changes in this flow-rate in liquid chromatographic systems have been suggested[1,2] to be leakage at the piston seal or check valve in a reciprocating piston pump, liquid compressibility under high pressure in a constant displacement pump, and carrier viscosity changes owing to changes in temperature and/or composition in a pneumatic amplifier pump. In addition to these factors, the column permeability, which is influenced by the settling and swelling of the packing in the column, and clogging in a line filter are also causes of changes in flow-rate. Further, in gradient elution chromatography, the composition of the carrier changes with time, which is accompanied by changes in viscosity and liquid volume. All of these factors adversely affect the analytical results.

Jackson and Henry introduced a feed-back flow controller in order to overcome these problems[3]. They employed a pressure transducer as a flow-sensing element, which monitors the pressure drop (Δp) across a calibrated flow restrictor. Therefore, their flow controller could not compensate for flow changes due to changes in viscosity and temperature.

In this study, the volumetric flow-rate of the carrier was measured at the outlet of the analytical column and this flow-rate was kept constant by using new electro-pneumatic flow controller. The design, characteristics and some applications of this flow controller in HPLC are described.

EXPERIMENTAL

Flow meter design

In order to eliminate viscosity-dependent characteristics involved in the method which monitors Δp across a flow restrictor, we employed a bubble flow tube, which is capable of measuring the volumetric flow-rate directly.

The flow meter is illustrated in Fig. 1. A very small air stream, for instance 40 μl/min, is introduced into the carrier flow through a small nozzle, and bubbles are formed periodically. The air line consists of a very narrow restrictor tube, a 60-m stainless-steel pipe of 0.08 mm I.D. and a pressure regulator that supplies a constant pressure of about 5–6 atm to this narrow restrictor tube so that the air flow-rate is kept constant, independent of changes in the carrier flow-rate and/or viscosity. With an aqueous carrier, bubbles are formed about every 20 sec and with methanol about every 5 sec.

The bubbles flow successively into a transparent flow tube (glass, 1 mm I.D.) and the time of travel between two points a definite distance apart on the flow tube (32 mm) is measured photoelectrically.

The inlet-side photo-transistor detects the entry of an air bubble into this flow tube by the change in intensity of the light from a light-emission diode, and starts the

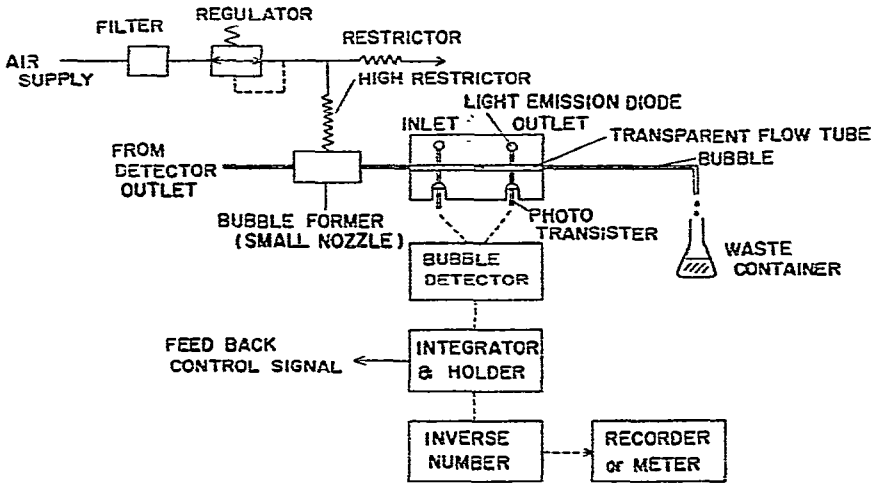

Fig. 1. The flow meter.

integrator circuit integrating a certain constant voltage with respect to time. The outlet-side photo-transistor detects the exit of the bubble and stops the integration. Thus, the integrator output voltage is proportional to the time of travel of the bubble and is inversely proportional to the sum of the bubble and carrier flow-rates.

The integrated voltage is held until the next bubble is measured and is used as the feed-back control signal. For direct reading purposes, this integrated voltage is converted into an inverse number. Then the air flow-rate, which has been measured independently, is subtracted from this inverted value to give the carrier flow-rate on a strip-chart recorder or a meter.

Flow control system

A pneumatic amplifier pump (Haskel, Burbank, Calif., U.S.A.) was used as the pumping system. In this constant-pressure system the carrier flow-rate changes slowly owing to a change in the column back-pressure (*i.e.*, caused by settling of the packing, or by swelling, etc.), or changes in the viscosity due to temperature or when solvent gradients are used. The time lag from the change in pressure of the air supply to the resulting carrier flow-rate change at the column outlet is relatively large. In view of these system characteristics and the fact that the flow-rate measurement is discontinuous, we employed a control system in which a control signal is fed back to re-set the setting of a precision pressure controller (booster relay) for the pneumatic amplifier pump. The control system is illustrated in Fig. 2 and a block diagram of the electronic control circuits is shown in Fig. 3.

As shown in Fig. 3, the flow-rate is set by using a digital switch in the voltage that is inversely proportional to the total flow-rate of the carrier and air. The integrator output voltage is compared with this pre-set voltage and the deviation is amplified in the differential amplifier circuit. This amplified deviation is fed to a motor drive circuit via a linearizer, which converts the deviation into a value proportional to the actual flow-rate deviation, and the motor is driven during the time proportional

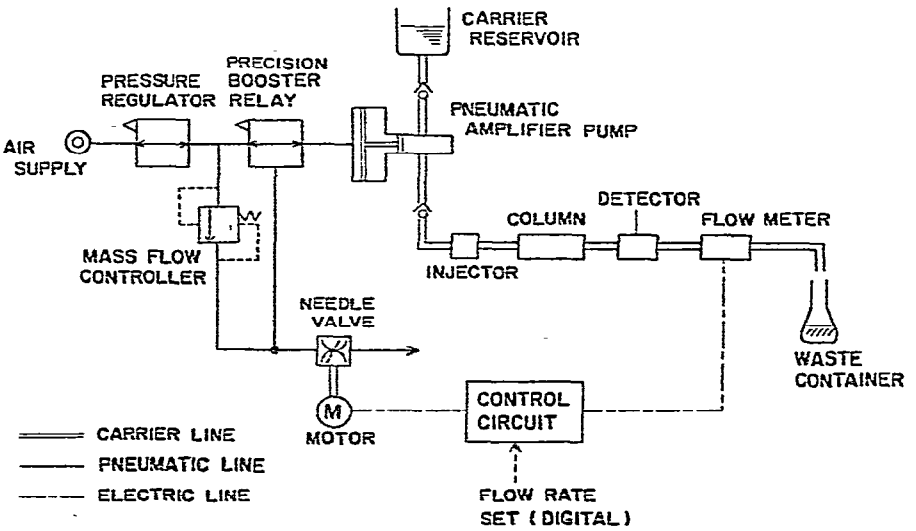

Fig. 2. Flow diagram of DuPont 830 liquid chromatograph with flow controller.

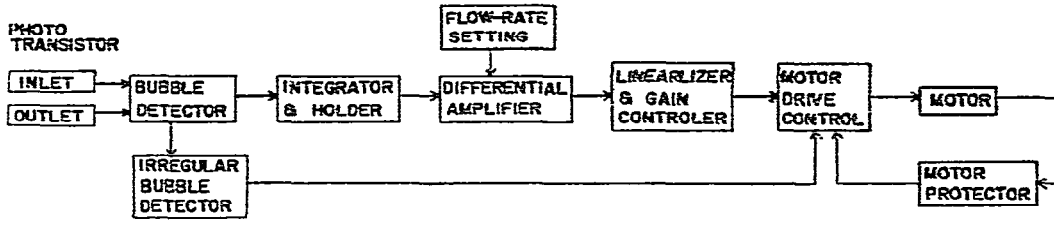

Fig. 3. Block diagram of electrical circuit for flow controller.

to the flow-rate deviation to rotate the needle valve shaft. The driving time can be adjusted by a gain controller.

As shown in Fig. 2, the needle valve is in the pneumatic control line. The pneumatic control line has a mass flow controller, a needle valve and a precision booster relay, and provides the following functions.

The mass flow controller always maintains a flow velocity of about 2 l/min, independent of the flow resistance of the needle valve. Hence the resistance change of the needle valve according to the shaft rotation by the motor causes a change in the inlet pressure of the needle valve. This pressure is supplied to the setting side of the precision booster relay to control the air pressure to the pneumatic amplifier pump so that the column inlet pressure is regulated so as to maintain the carrier flow-rate constant.

As described above, there is some time delay in the control loop and the measurement of the flow-rate is discontinuous. Therefore, the amount of feed-back must be suppressed so as to follow the set flow-rate gradually. The relationships between the kind of carrier and the amount of feed-back were carefully examined.

Liquid chromatograph

The liquid chromatograph used was a DuPont Model 830 instrument equipped with gradient elution accessories. A photograph of the combined Model 830 instrument and the flow controller (on the left) is shown in Fig. 4.

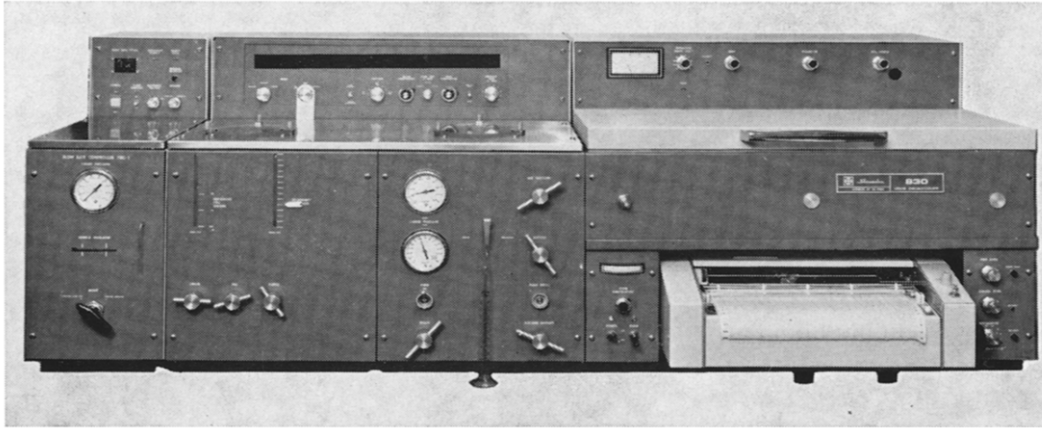

Fig. 4. Liquid chromatograph with flow controller (left-hand module).

The liquid chromatographic column (1 m × 2.1 mm I.D.) was packed with Permaphase ODS (DuPont, Wilmington, Del., U.S.A.). The carriers were distilled water and reagent-grade methanol. The samples were fused-ring aromatic hydrocarbon standards such as naphthalene, biphenyl, anthracene, pyrene, chrysene and benzo[*a*]pyrene. Sample injections were made with a high-pressure sampling valve. The sample volume was 12 μl.

Other equipment

A Model ITG-4A and Chromatopac-1A (Shimadzu Seisakusho Ltd., Kyoto, Japan) digital integrator was used. In addition to a DuPont gradient programmer, a Model GRE-1 multi-linear gradient programmer (Shimadzu Seisakusho Ltd.) was also used.

RESULTS AND DISCUSSION

Flow-rate measurement and control

In the flow meter, if the back-pressure at the air-bubble former (nozzle) is changed, the air flow-rate is also changed and this change causes an error in the measurement of the carrier flow-rate. In order to avoid this erroneous measurement, it is necessary to keep the back-pressure as low as possible and to take precautions so that the influence of the change in back-pressure is as small as possible. In this study, the back-pressure was kept as low as 0.01 kg/cm^2, and the air pressure supply was as high as 5 kg/cm^2. Hence the air flow-rate was maintained constant.

It was observed that in the measurement of flow-rate, the resistance change in the narrow restrictor tube and the change in the length of the flow tube by fluctuations in the ambient temperature were negligibly small.

The relationship between the set flow-rate and the real flow-rate controlled by the flow controller is shown in Table I. The real flow-rate was measured by the gravimetric method using water as carrier. The linearity is better than approximately 1% in the range from 1.0 to 4.5 ml/min in water. As a result, the controller is capable of covering a range from 0.3 to 4.9 ml/min.

TABLE I

RELATION BETWEEN SET FLOW-RATE AND REAL FLOW-RATE

Carrier, water; bubble interval, about 20 sec.

Set flow-rate (ml/min)	*Real flow-rate (ml/min)*	*Deviation (%)*
1.0	0.995	0.5
2.0	2.020	1.0
3.0	3.024	0.8
4.5	4.524	0.5

Fig. 5 shows an example of actual control functions. It shows the recorder trace of 0.8 ml/min of water with the full scale of recorder set to 1 ml/min. The results indicate that the flow-rate is controlled to within ± 0.2–0.3% of the set flow-rate.

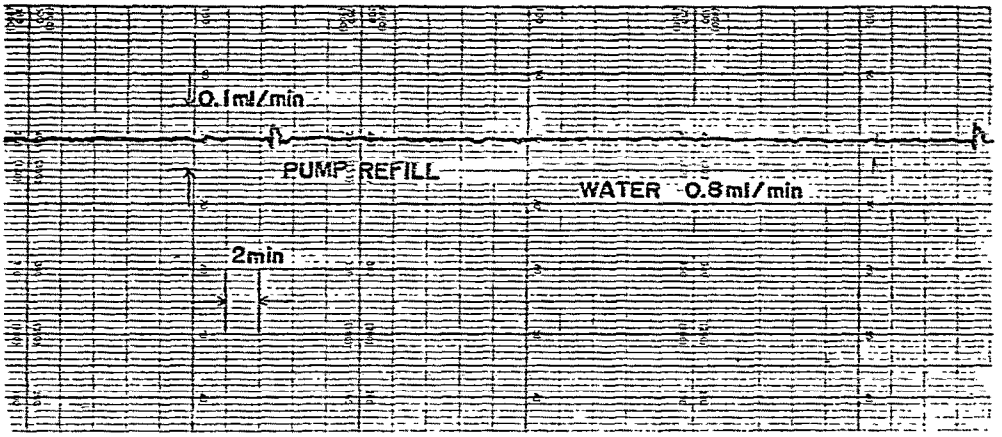

Fig. 5. Example of flow-rate record. One division corresponds to 0.01 ml/min.

Application in isocratic elution chromatography

Fig. 6 is an example of a high-performance liquid chromatogram of fused-ring aromatic hydrocarbon standards obtained by using a Model 830 liquid chromatograph equipped with the flow controller. The flow-rate was also recorded simultaneously. Five peaks were recorded in the order solvent, unknown, biphenyl, an-

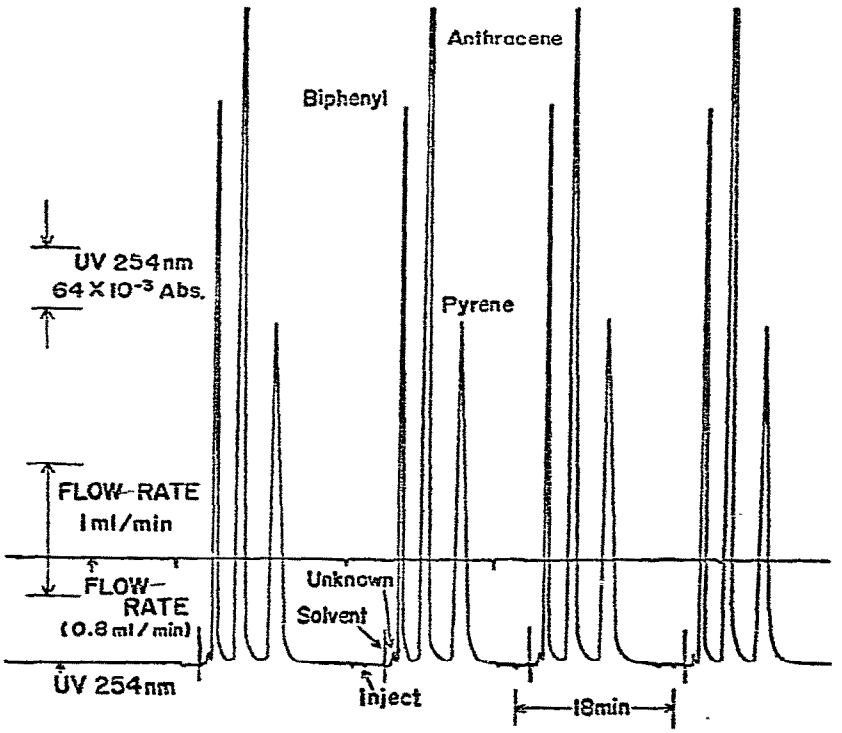

Fig. 6. Chromatogram for reproducibility check. Operating conditions: column, Permaphase ODS, 1 m × 2.1 mm I.D.; temperature, 50°; carrier, methanol–water (3:2); flow-rate, 0.8 ml/min; detector, UV photometer (254 nm) at $64 \cdot 10^{-2}$ a.u.f.s.

TABLE II

REPRODUCIBILITY OF RETENTION TIME IN ISOCRATIC ELUTION

Column, Permaphase ODS, 1 m × 2.1 mm I.D.; temperature, 50°; carrier, methanol–water (3:2); flow-rate, 0.8 ml/min; detector, UV photometer at 254 nm.

Run No.	*Retention time (min)*				
	Solvent	*Unknown*	*Biphenyl*	*Anthracene*	*Pyrene*
1	1.63	2.80	3.54	6.51	10.64
2	1.64	2.81	3.55	6.52	10.64
3	1.64	2.81	3.55	6.50	10.61
4	1.64	2.81	3.55	6.50	10.61
5	1.65	2.81	3.55	6.50	10.62
6	1.65	2.82	3.55	6.51	10.63
7	1.65	2.81	3.55	6.51	10.62
8	1.65	2.81	3.55	6.51	10.62
9	1.64	2.81	3.54	6.51	10.62
10	1.65	2.81	3.55	6.51	10.63
11	1.65	2.82	3.56	6.52	10.66
12	1.64	2.81	3.55	6.52	10.65
Average	1.6442	2.8108	3.5492	6.52	10.629
σ	0.0064	0.00493	0.00493	0.00707	0.01439
Coefficient of variation	0.39%	0.175%	0.139%	0.109%	0.141%

thracene and pyrene. The carrier was 60% methanol in water. A UV 254 absorption detector was used at the full-scale range of $64 \cdot 10^{-2}$ absorbance unit. The flow-rate was 0.8 ml/min. Under such conditions, the reproducibilities of the retention time and peak area were determined and the results are shown in Tables II and III.

TABLE III

REPRODUCIBILITY OF PEAK AREA IN ISOCRATIC ELUTION

Operating conditions as in Table II.

Run No.	*Peak area ratio*	
	Biphenyl/anthracene	*Pyrene/anthracene*
1	0.4228	0.6751
2	0.4206	0.6747
3	0.4204	0.6864
4	0.4176	0.6738
5	0.4179	0.6740
6	0.4194	0.6773
7	0.4187	0.6753
8	0.4161	0.6703
9	0.4168	0.6717
10	0.4172	0.6745
11	0.4199	0.6758
12	0.4159	0.6710
Average	0.4186	0.6750
σ	0.00197	0.00395
Coefficient of variation	0.472%	0.585%

It can be seen from Table II that the reproducibility of the retention time was excellent. The coefficients of variation were 0.39% for the solvent peak, 0.175% for the unknown peak, 0.139% for biphenyl, 0.109% for anthracene and 0.141% for pyrene.

The reproducibility of the peak area measured by a digital integrator (Shimadzu ITG-4A) is shown in Table III. The reproducibilities of the peak area ratio of biphenyl to anthracene and pyrene to anthracene are 0.472 and 0.585% (coefficients of variation), respectively.

Application in gradient elution chromatography

The change in flow-rate in gradient elution chromatography using the flow controller is shown in Fig. 7. In this instance the carrier was varied from 100% water to 100% methanol at a gradient rate of 5%/min. As can be seen from Fig. 7, the flow-rate is kept constant even in the gradient elution operation. Thus, the gradient elution chromatography is carried out with no effect from changes in flow-rate, and the separation is expected to be governed only by the characteristics of the solvent.

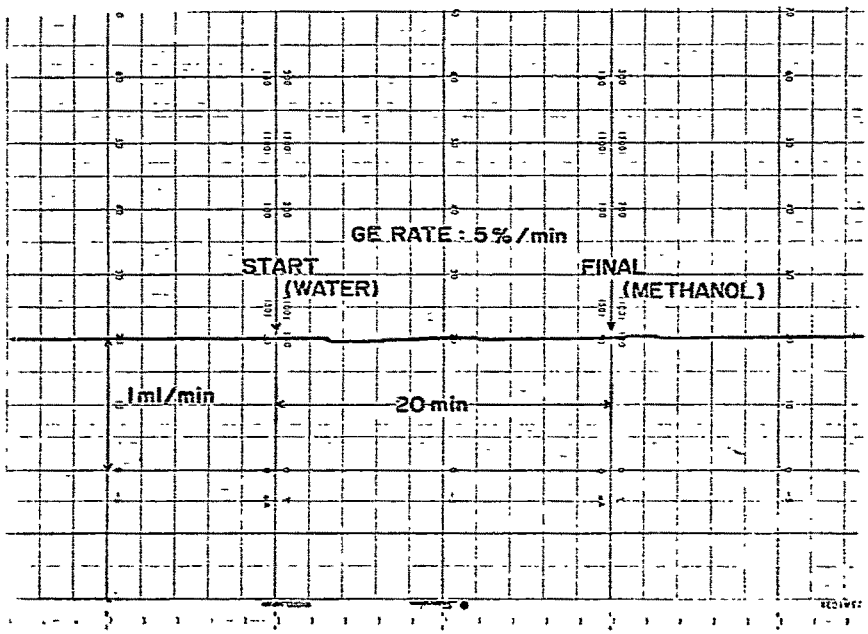

Fig. 7. Flow-rate during gradient elution using flow controller. Operating conditions: column, Permaphase ODS, 1 m × 2.1 mm I.D.; temperature, 50°, carrier, from 100% water to 100% methanol at the rate of 5%/min.

Table IV illustrates the reproducibility of the retention times in gradient elution chromatography. This analysis was carried out in 2 days and the results demonstrate that a reproducibility of better than 0.3% is obtained for all peaks.

Constant flow operations in gradient elution chromatography have a great advantage in quantitative analysis. The effects of the gradient rate on peak retention

TABLE IV

REPRODUCIBILITY OF RETENTION TIME IN GRADIENT ELUTION

Column, Permaphase ODS, 1 m × 2.1 mm I.D.; temperature, 50°; carrier, from 100% water to 100% methanol at the rate of 4%/min; flow-rate, 1.0 ml/min; detector, UV (254 nm) at $64 \cdot 10^{-2}$ a.u.f.s.

Run No.	*Retention time (min)*						
	Naphthalene	*Biphenyl*	*Anthracene*	*Pyrene*	*Chrysene*	*Benzo[e]-pyrene*	*Benzo[a]-pyrene*
1	12.38	16.08	19.22	21.72	23.69	25.53	25.91
2	12.33	16.09	19.25	21.74	23.69	25.50	25.92
3	12.47	16.23	19.35	21.82	23.75	25.54	25.94
4	12.42	16.17	19.28	21.79	23.70	25.50	25.90
5	12.38	16.19	19.28	21.78	23.72	25.52	25.91
6	12.39	16.18	19.31	21.77	23.71	25.50	25.89
7	12.37	16.14	19.26	21.76	23.66	25.44	25.86
8	12.35	16.12	19.25	21.72	23.17	21.41	25.83
9	12.35	16.12	19.23	21.75	23.69	25.47	25.88
10	12.38	16.13	19.22	21.69	23.69	25.43	25.85
Average	12.383	16.145	19.265	21.753	23.687	25.484	25.889
σ	0.038	0.045	0.039	0.037	0.036	0.042	0.032
Coefficient of variation	0.307%	0.276%	0.204%	0.172%	0.168%	0.166%	0.125%

time and area are shown in Tables V, VI and VII. The gradient rate examined is also shown in Fig. 8. For the purpose of comparison, the effects of carrier composition on retention time and area in isocratic elution chromatography are shown in Table VIII and the chromatogram is shown in Fig. 9.

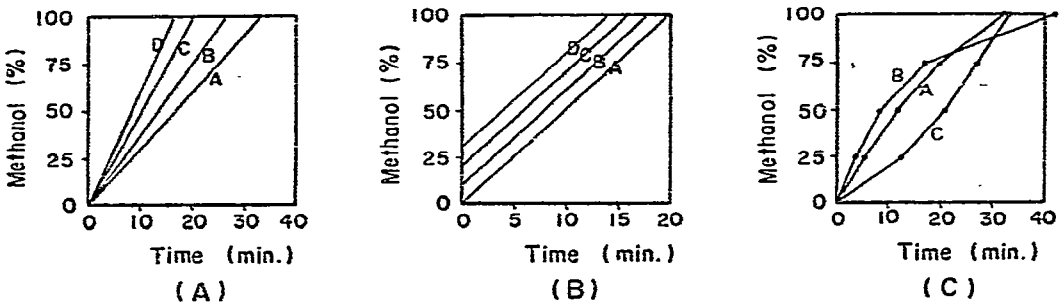

Fig. 8. Gradient function.

It was observed clearly that the effect of changes in the carrier composition on the peak area is fairly small. Therefore, when the concentration-sensitive detector (*e.g.*, a UV absorption detector) is used, the re-calibration procedures associated with gradient rate change can be expected to be eliminated.

TABLE V

EFFECTS OF GRADIENT RATE ON RETENTION TIME AND PEAK AREA

Column, Permaphase ODS, 1 m × 2.1 mm I.D.; temperature, 55°; detector, UV (254 nm); carrier, methanol added to water (from 0 to 100%); flow-rate, 0.8 ml/min. Gradient rate: A, 3%/min; B, 4%/min; C, 5%/min; D, 6%/min (as shown in Fig. 8A).

Gradient function	*Naphthalene*		*Biphenyl*		*Anthracene*		*Pyrene*		*Chrysene*		*Benzo[a]pyrene*	
	t_R*	*Area***	t_R*	*Area***	t_R*	*Area***	t_R*	*Area***	t_R*	*Area***	t_R*	*Area***
A	1496	11158	1836	10324	2131	68230	2311	9278	2478	18466	2685	10798
B	1317	10806	1563	10701	1778	66682	1915	9710	2038	18906	2195	10755
C	1165	10876	1352	10330	1517	63698	1622	9143	1717	17930	1839	10116
D	1079	15740	1229	10301	1372	64549	1464	9433	1542	18415	1645	10263
Average		10947		10414		65790		9396		18429		10483
σ		152		166		1779		142		345		298
Coefficient of variation		1.39%		1.59%		2.70%		2.21%		1.87%		2.84%

* t_R = retention time; 1/100 min.

** Area = area counts measured with Chromatopac 1A.

TABLE VI

EFFECTS OF INITIAL CONCENTRATION ON RETENTION TIME AND PEAK AREA

Operating conditions are as in Table V except for the initial concentration and gradient rate. Gradient rate, 5%/min. Gradient: A, 0–100%; B, 10–100%; C, 20–100%; D, 30–100% (as shown in Fig. 8B).

Gradient function	*Naphthalene*		*Biphenyl*		*Anthracene*		*Pyrene*		*Chrysene*		*Benzo[a]pyrene*	
	t_R*	*Area***	t_R*	*Area***	t_R*	*Area***	t_R*	*Area***	t_R*	*Area***	t_R*	*Area***
A	1165	10876	1352	10330	1517	63698	1622	9143	1717	17930	1839	10116
B	971	10887	1155	10284	1331	66915	1443	9174	1541	18213	1665	10558
C	794	11360	975	10135	1145	64380	1254	9027	1345	17985	1475	10425
D	587	11379	760	10106	932	64430	1042	8917	1140	18607	1270	10807
Average		11125.5		10213.8		14855.8		9065.3		18183.8		10476.5
σ		244		95		280		101		266		249
Coefficient of variation		2.194%		0.932%		1.887%		1.121%		1.465%		2.379%

* t_R = retention time; 1/100 min.

** Area = area counts measured with Chromatopac 1A.

TABLE VII

EFFECTS OF GRADIENT RATE ON RETENTION TIME AND PEAK AREA

Operating conditions as in Table V except for the gradient function: A, 0–25% at 5%/min; 25–50% at 4%/min, 50–75% at 3%/min, 75–100% at 2%/min; B, 0–25% at 7%/min, 25–50% at 5%/min, 50–75% at 3%/min, 75–100% at 1%/min; C, 0–25% at 2%/min, 25–50% at 3%/min, 50–100% at 4%/min (as shown in Fig. 8C).

Gradient function	*Naphthalene*		*Biphenyl*		*Anthracene*		*Pyrene*		*Chrysene*		*Benzo[a]pyrene*	
	t_R*	*Area***	t_R*	*Area***	t_R*	*Area***	t_R*	*Area***	t_R*	*Area***	t_R*	*Area***
A	1201	10771	1426	10097	1646	63658	1805	9134	1961	16758	2166	10885
B	1061	10392	1233	10037	1433	65231	1583	8785	1731	16326	1924	10340
C	1823	10623	2228	9908	2535	64191	2702	9289	2845	18498	3015	10324
Average		10595		10014		64360		9069		17194		10522
σ		156		78.9		653		210		938		280
Coefficient of variation		1.47%		0.78%		1.01%		2.32%		5.45%		2.66%

* t_R = retention time; 1/100 min.
** Area = area counts measured with Chromatopac 1A.

TABLE VIII

EFFECTS OF METHANOL CONCENTRATION ON RETENTION TIME AND PEAK AREA

Column, Permaphase ODS, 1 m × 2.1 mm I.D.; temperature, 55°; detector, UV (254 nm); carrier, methanol added to water.

Methanol (%)	*Naphthalene*		*Biphenyl*		*Anthracene*		*Pyrene*		*Chrysene*		*Benzo[a]pyrene*	
	t_R*	*Area***	t_R*	*Area***	t_R*	*Area***	t_R*	*Area***	t_R*	*Area***	t_R*	*Area***
40	374	10779	613	10231	1253	69962	2239	8571	4453	16625	10506	9752
45	304	11033	447	10256	822	69995	1372	8804	2479	17176	5306	9685
50	255	10674	339	9934	559	69231	869	8829	1445	17363	2905	10337
55	218	—***	268	—***	396	67884	569	8975	862	17261	1619	10389
60	196	—***	226	—***	305	—***	411	8498	574	18271	999	10547
Average		10804		10064		69035		8799		17344		10282
σ		137		182		890		214		484		306
Coefficient of variation		1.271%		1.819%		1.298%		2.430%		2.797%		2.989%

* t_R = retention time; 1/100 min.
** Area = area counts measured with Chromatopac 1A.
*** These peaks were not separated from neighbouring peaks.

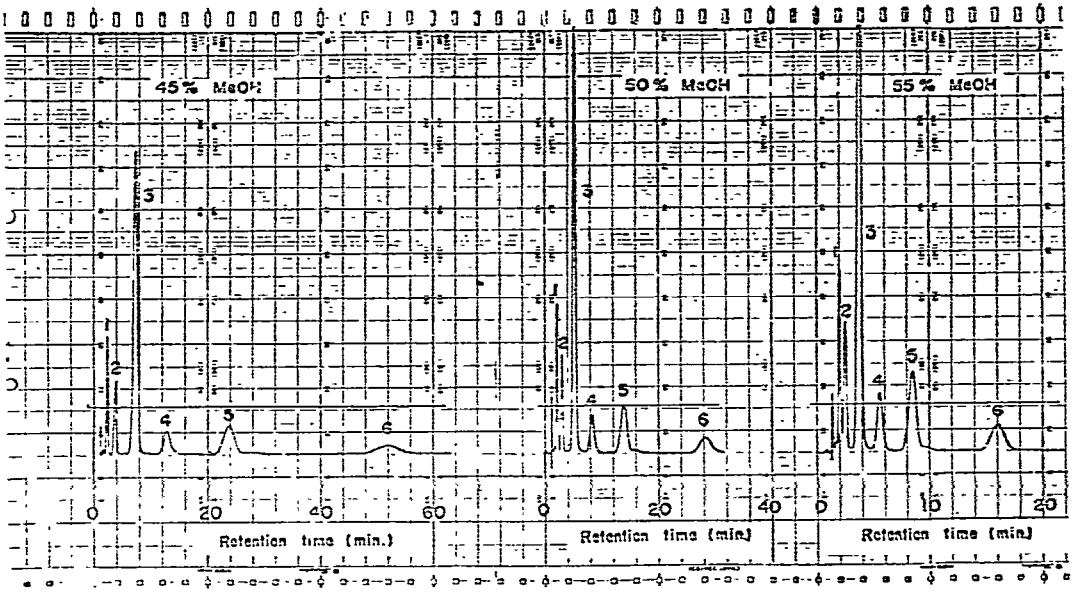

Fig. 9. Influence of carrier composition on peak retention time and area. Operating conditions: column, Permaphase ODS, 1 m × 2.1 mm I.D.; temperature, 55°; mobile phase, methanol–water (0.8 ml/min); detector, UV 254. Peaks: 1, naphthalene; 2, biphenyl; 3, anthracene; 4, pyrene; 5, chrysene; 6, benzo[*a*]pyrene.

ACKNOWLEDGEMENTS

The authors are grateful to Dr. T. Haruki for his helpful advice on this work, and to Dr. K. Okamoto for technical assistance.

REFERENCES

1 L. Berry and B. L. Karger, *Anal. Chem.*, 45 (1973) 819A.
2 M. Martin, G. Blu, C. Eon and G. Guiochon, *J. Chromatogr.*, 112 (1975) 399.
3 M. T. Jackson and R. A. Henry, *Int. Lab.*, Nov./Dec. (1974) 57.